12-1-2019

Impact of nonlinear chemical reaction and melting heat transfer on an MHD nanofluid flow over a thin needle in porous media

Muhammad Ramzan
Bahria University

Hina Gul
Bahria University

Seifedine Kadry
Beirut Arab University

Chhayly Lim
Soonchunhyang University

Yunyoung Nam
Soonchunhyang University

See next page for additional authors

applied sciences

MDPI

Article

Impact of Nonlinear Chemical Reaction and Melting Heat Transfer on an MHD Nanofluid Flow over a Thin Needle in Porous Media

Muhammad Ramzan [1,2,*], Hina Gul [1], Seifedine Kadry [3], Chhayly Lim [4], Yunyoung Nam [5,*] and Fares Howari [6]

1 Department of Computer Science, Bahria University, 44000 Islamabad, Pakistan; gulhina7766@gmail.com
2 Department of Mechanical Engineering, Sejong University, Seoul 143747, Korea
3 Department of Mathematics and Computer Science, Faculty of Science, Beirut Arab University, Beirut 115020, Lebanon; skadry@gmail.com
4 Department of ICT Convergence Rehabilitation Engineering, Soonchunhyang University, Asan 36538, Korea; chaylylim@gmail.com
5 Department of Computer Science and Engineering, Soonchunhyang University, Asan 36538, Korea
6 College of Natural and Health Sciences, Zayed University, 144543 Abu Dhabi, UAE; Fares.Howari@zu.ac.ae
* Correspondence: mramzan@bahria.edu.pk (M.R.); ynam@sch.ac.kr (Y.N.)

Received: 20 November 2019; Accepted: 11 December 2019; Published: 13 December 2019

Abstract: A novel mathematical model is envisioned discussing the magnetohydrodynamics (MHD) steady incompressible nanofluid flow with uniform free stream velocity over a thin needle in a permeable media. The flow analysis is performed in attendance of melting heat transfer with nonlinear chemical reaction. The novel model is examined at the surface with the slip boundary condition. The compatible transformations are affianced to attain the dimensionless equations system. Illustrations depicting the impact of distinct parameters versus all involved profiles are supported by requisite deliberations. It is perceived that the melting heat parameter has a declining effect on temperature profile while radial velocity enhances due to melting.

Keywords: nonlinear chemical reaction; thin needle; melting heat transfer; MHD

1. Introduction

The study of magnetohydrodynamics (MHD) explains the magnetic features of electrically conducting fluids. Normally, it affects the heat transfer and appears as Joule heating and Lorentz force. Cooling of the refrigerator, saltwater, plasma, tumor therapy, radiation of X-ray, and electrolytes are examples of MHD. Many valuable works done have been published highlighting varied aspects of MHD. Hayat et al. [1] highlight the unsteady MHD nanoliquid flow over a starching sheet in the attendance of viscous dissipation and stratification. Ramzan et al. [2] discussed steady MHD Jeffery nanofluid flow over a vertical inclined cylinder with chemical reaction, thermal radiation, and double stratification. They engaged the homotopy analysis method (HAM) to obtain series solutions. Shehzad et al. [3] discussed the impact of viscous dissipation on tangent hyperbolic non-Newtonian fluid over a stretching sheet with Joule heating. They obtained results by implementing numerical procedure (Keller-box method). They also examined that the fluid velocity is lowered by enlarging the Weissenberg number. Some more recent remarkable researches featuring MHD may be found at [4–7] and many therein.

The increasing rate of heat transfer by employing nanofluid rather than the real base fluids has attracted the attention of researchers around the world, which makes a clear difference between nanofluids and the base fluid. Nanofluids holding nanoparticles submerged into the base fluid are

termed as coolants to increase the heat transfer functioning in power generators, nuclear reactors, manufacturing paper, electronic devices, domestic refrigerators, air conditioning, and the automotive industry. Choi [8] first floated the idea of nanofluid and discloses that the thermal properties of the base fluids are greatly improved once the nanoparticles are incorporated into them. After this significant effort, many researchers talked about the implications of the nanoparticles supplement to the fluid flows. Choi's results are verified experimentally by Kang et al. [9]. Jafaryar et al. [10] debated nanofluid heat transfer in the pipe with twisted tape with an alternative axis. They engaged the finite volume method as a simulation tool. They also demonstrated the influence of Reynold number and revolution angle on nanofluid hydrothermal treatment. Hayat et al. [11] scrutinized the variable heat flux with stagnation point nanofluid flow over a thin needle. They used ND shooting technique for solving differential equations numerically. They also examined that the velocity profile increases for greater estimation of nanoparticles volume fraction. Nonlinear thermal radiation nanomaterial flow with viscous dissipation over a thin moving needle is discussed by Khan et al. [12]. They employed the second law of thermodynamics for entropy generation minimization (EGM). For greater values of radiative parameters, the lowest heat transfer rate is observed. The effect of Joule heating in MHD Sakiadis flow with Brownian motion and thermophoresis on a continuously moving thin needle is investigated by Sulochana et al. [13]. Some recent explorations regarding nanofluid flows over a thin needle are given at [14–16].

The basic theory of Navier–Stokes is the no-slip boundary condition that is explored by many researchers under certain conditions. There are some applications where no-slip conditions are not applicable and change to partial slip condition. The boundary slip has many uses, like artificial heart valves and polished internal cavities, which are valuable examples of slip. Because of the wide scope of applications, scientists and researchers have focused nowadays on heat transfer and flow analysis at a micro-scale, which are interconnected to the slip effects. Khaled and Vafai [17] discussed the combined effect of Stokes and Couette flows with slip condition on the oscillating wall. They reported that for the Stokes flow the transient velocity reduces due to wall slip while transient effects are minimum for Couette flow. This is obtained only for higher and lower estimation of the wall slip and the gap thickness, respectively. Wang and Chiu [18] discussed the result of slip condition analytically and numerically. The numerical solution for Newtonian liquid flow over an impermeable stretching sheet with slip velocity, variable thickness, and power-law surface velocity was discussed by Khader and Megahed [19]. Bhattacharyya et al. [20] observed the slip effect with mixed convective boundary layer flow induced by a flat plate.

The idea of porous media is employed in many areas of engineering and applied science such as mechanics, filtration, petroleum engineering, construction engineering, hydrogeology, geophysics, petroleum geology, biology, and biophysics. Sheikholeslami [21] investigated the MHD nanoliquid flow inside the porous cavity. He employed the control-volume finite element method (CVFEM) to simulate the behavior of a magnetic field. Entropy generation under the effect of MHD nanofluid through porous media is also reported by Sheikholeslami [22]. Some more researches about porous media are given at [23–25].

The phenomenon of melting heat has gained the attention of scientists and researchers due to its ample applications in innovative industrial and technological processes. In the last few years, scientists have focused on developing more sustainable, competent, and cheap energy storage technologies. Such technologies are connected to unwanted heat recovery, solar energy, heat plants, and power. The behavior of melting heat transfer in a warm air stream of ice slab was first portrayed by Robert [26]. The effect of melting heat transfer and mixed convection in the flow of Maxwell fluid generated by linear stretching surface debated by Hayat et al. [27]. Das [28] examined the deformation of MHD flow of viscous fluid produced by a moving surface with melting effect and thermal radiation. The effect of the boundary layer with melting heat transfer nanofluid flow due to a stretching surface with the magnetic field is analyzed by Mabood [29].

As the above-referred survey discloses, there are abundant studies available discussing the flow of nanofluids in varied scenarios with different geometries; however, less material exists conversing the nanofluid flows over thin needles. This channel becomes even narrower when we talk about nanofluid flow over a thin needle with the simultaneous impacts of melting heat and nonlinear chemical reaction in permeable media. The layout of the subject mathematical model consists of, firstly, the erection of the mathematical model. Secondly, the detail of the numerical scheme concerns the presented model. Thirdly, the results and discussion section and, lastly, the conclusions.

2. Mathematical Modeling

Assume an MHD steady, a thin needle immersed is in a nanofluid with a uniform stream velocity u_∞ of incompressible flow with permeable media in the existence of viscous dissipation and temperature-dependent heat sink/source. The effects of melting heat transfer and non-linear chemical reactions are also considered with the slip boundary. The strength of magnetic field B_0 is applied in the radial direction. Here, induced magnetic and electric fields are neglected due to our presumption of a small value of Reynolds number. The needle is seen as thin and its thickness is smaller than the boundary layer formed over it. A physical interpretation of the flow can be seen in Figure 1. Here, $x-$ coordinate is measured as the axial and $r-$ as the radial direction of the cylinder. Assume the function $r = R(x) = (vxc/U)^{1/2}$ determines the state of a slight needle in which $U = u_w + u_\infty$ is the composite velocity.

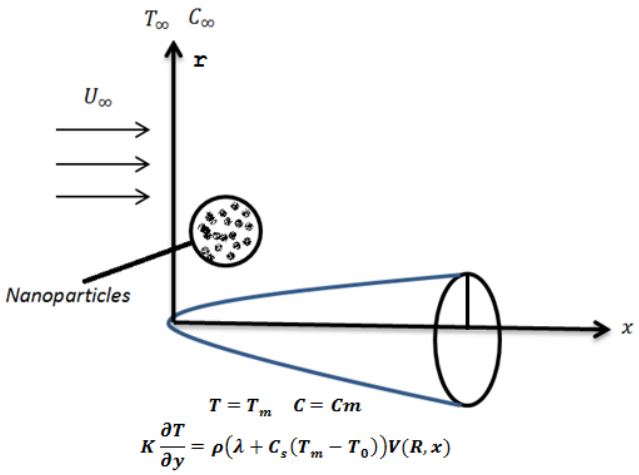

Figure 1. Geometrical sketch of the model.

The boundary layer governing equations are represented as:

$$ru_x + ur_x + vr_r + rv_r = 0, \tag{1}$$

$$uu_x + vu_x = \frac{v}{r}(ru_{rr} + u_r r_r) - \frac{\sigma B_0^2 u}{\rho} - \frac{v}{k^*}u, \tag{2}$$

$$uT_x + vT_r = \frac{\alpha}{r}(rT_{rr} + T_r r_r) + \tau\left(D_B T_r C_r + \frac{D_T}{T_\infty}(T_r)^2\right) + \frac{Q_0}{(\rho c_p)_f}(T - T_m) + \frac{\sigma B_0^2 u^2}{(\rho c_p)_f}, \tag{3}$$

$$uC_x + vC_r = \frac{D_B}{r}(rC_{rr} + C_r r_r) + \frac{D_T}{T_\infty}\frac{1}{r}(rT_{rr} + T_r r_r) - K_n(C - C_m)^n. \tag{4}$$

The suitable boundary conditions are described by:

$$\begin{gathered} u = u_w + L u_r|_{r=0},\ T = T_m, C = C_m, \text{at } r = R(x) \\ u \to u_\infty,\ \ T \to T_\infty,\ \ C \to C_\infty,\ \ \text{as } r \to \infty, \\ K(T_r)_{r=R} = \rho(\lambda_1 + C_s(T_m - T_0))v(R,x). \end{gathered} \tag{5}$$

Similarity transformations are defined as:

$$\psi = vxf(\eta), \theta(\eta) = \frac{T - T_m}{T_\infty - T_m}, \varphi(\eta) = \frac{C - C_m}{C_\infty - C_m}, \eta = \frac{Ur^2}{vx}. \tag{6}$$

Using the above transformation, the incompressibility Equation is satisfied, and Equations (2)–(4) are transformed into:

$$2\eta f''' + 2f'' + ff'' - \frac{1}{2}\lambda f'\left(M^2 + k_0\right) = 0, \tag{7}$$

$$\frac{2}{\mathrm{Pr}}(\theta' + \eta\theta'') + 2\eta\left(N_b\theta'\varphi' + N_t\theta'^2\right) + f\theta' + \frac{\lambda}{2}M^2 f'^2 + \frac{\lambda}{2}Q\theta = 0, \tag{8}$$

$$2(\eta\varphi'' + \varphi') + 2\frac{N_t}{N_B}(\eta\theta'' + \theta) + Scf\varphi' - \frac{\lambda}{2}\gamma\phi^n = 0. \tag{9}$$

The pertinent boundary conditions are:

$$\begin{gathered} \text{At } \eta = m; f' = \tfrac{\lambda}{2} + \tfrac{2}{\sqrt{\lambda}}S_1\eta f'', \theta = 0, \varphi = 0, \\ \text{As } \eta = \infty; f' \to \tfrac{1-\lambda}{2}, \theta \to 1, \varphi \to 1, \\ M_e\theta' + \tfrac{\mathrm{Pr}}{\eta}(f - \eta f') = 0. \end{gathered} \tag{10}$$

With

$$\begin{gathered} \mathrm{Pr} = \frac{\upsilon}{\alpha},\ Sc = \frac{\upsilon}{D_B},\ N_t = \frac{\tau D_T\left(T_\infty - T_m\right)}{\upsilon T_\infty},\ N_b = \frac{\tau D_B C_\infty}{\upsilon T_\infty},\ S_1 = L\sqrt{\frac{1}{\nu}}, \\ \gamma = \tfrac{K_n C_\infty^{n-1}}{c}, M^2 = \tfrac{\sigma B_0^2}{\rho c}, M_e = \tfrac{c_p(T_\infty - T_m)}{\lambda_1 + C_s(T_m - T_0)}, \lambda = \tfrac{u_w}{(u_w + u_\infty)}. \end{gathered} \tag{11}$$

The heat transfer rate and skin friction are classified by:

$$\tau_{wx} = \tau_{rx}|_{r=R(x)} = \mu_f u_r|_{r=R(x)} = \frac{4mU^2}{v_f x}f''(m), Nu = \frac{xq_w}{k(T_\infty - T_m)}, \tag{12}$$

where

$$q_w = -kT_z|_{z=0}. \tag{13}$$

Through the transformations defined in Equation (5), the drag force and heat transfer rate in dimensionless form are appended below:

$$C_f = \frac{\tau_{wx}}{\rho U^2} = 4\mathrm{Re}_x^{1/2}m^{1/2}f''(m), Nu = -2\mathrm{Re}_x^{1/2}m^{1/2}\theta'(m), \tag{14}$$

where

$$\mathrm{Re}_x = \frac{xU}{\nu_f}. \tag{15}$$

3. Numerical Method

In the current model, the MATLAB built-in-function bvp4c is used to solve coupled ordinary differential equations (ODEs) (Equations (7)–(9)) with mentioned boundary conditions (Equation (10)). For computational purposes, the infinite domain is restricted to $\eta = 4$, which is enough to indicate the asymptotic behavior of the solution. The theme numerical scheme needs initial approximation with

tolerance 10^{-6}. The initially taken estimation must meet the boundary conditions without interrupting the solution technique.

$$
\begin{aligned}
&f = y_1,\\
&f\prime = y_2,\\
&f'' = y_3,\\
&f''' = yy_1\\
&yy_1 = \tfrac{-1}{2\eta}(2y_3 + y_1y_3 - \tfrac{1}{2}\lambda y_2(M^2 + k_0),\\
&\theta = y_4,\\
&\theta\prime = y_5,\\
&\theta'' = yy_2,\\
&yy_2 = \tfrac{-\mathrm{Pr}}{2\eta}(2\eta\left(N_b y_5 y_7 + N_t y_5^2\right) + y_2y_5 + \tfrac{\lambda}{2}M^2y_2^2 + \tfrac{\lambda}{2}Qy_4 + \tfrac{2}{\mathrm{Pr}}y_5,\\
&\varphi = y_6,\\
&\varphi\prime = y_7,\\
&\phi'' = yy_3,
\end{aligned}
$$

$$yy_3 = \frac{-1}{2\eta}(2y_7 + 2\frac{N_t}{N_b}(\eta yy_2 + y_4) + Scy_1y_7 - \frac{\lambda}{2}\gamma y_6. \tag{16}$$

With associated boundary conditions:

$$
\begin{aligned}
&y_2 = \tfrac{1}{2}\lambda + \tfrac{2}{\sqrt{\lambda}}S_1\eta y_3, y_4 = 0, y_6(0) = 0,\\
&y_2 = \tfrac{1-\lambda}{2}, y_4 = 1, y_6 = 1,\\
&M_e y_5 + \tfrac{\mathrm{Pr}}{\eta}(y_1 - \eta y_2).
\end{aligned} \tag{17}
$$

4. Results and Discussion

This segment is prepared to investigate the impacts of involved parameters $M, \lambda, Q, \mathrm{Pr}, N_t, N_b, \gamma, M_1, k_0$ and Sc on dimensionless velocity, temperature and concentration, Nusselt number, and skin friction coefficient. The influence of the velocity ratio parameter (λ) on velocity distribution is drawn in Figure 2. It is observed that when $0 < \lambda < 0.5$, the axial velocity expands just close to the surface of the needle and diminishes far from it. However, a contrary pattern is noticed for the values of ratio parameter greater than zero.

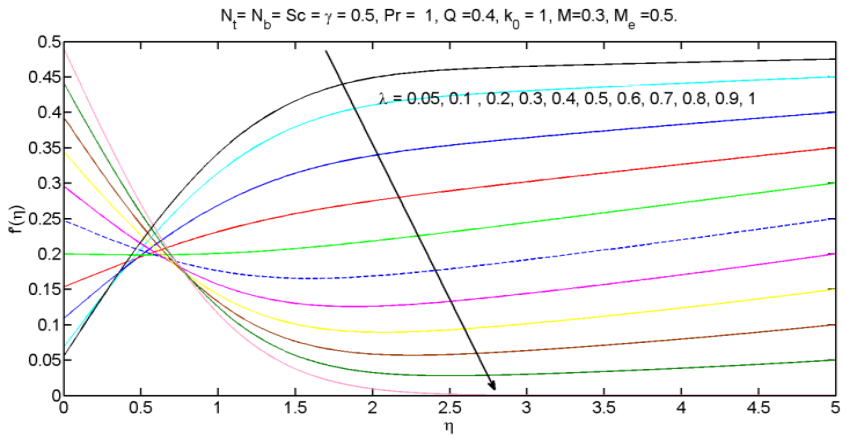

Figure 2. Illustration of $f'(\eta)$ versus λ.

Figure 3 portrays the impact of different estimations of the velocity ratio parameter (λ) on the temperature profile. It is witnessed that for escalating values of ratio λ, the temperature profile is enhanced. In Figure 4, the output of λ on the nanoparticle concentration profile is demonstrated. It is examined that for mounting values of λ, the concentration profile $\varphi(\eta)$. decreases. Figure 5 reveals the needle velocity for various estimations of the melting parameter (M_e). It is examined that for the mounting valuation of M_e, the velocity profile increases. For a stronger M_e, more molecular motion is observed, thus increasing the fluid velocity. In Figure 6, a variation of the magnetic parameter (M) on the velocity field is portrayed. It is found that an increase in (M) causes a decreased velocity profile. Sturdier Lorentz force hinders the movement of the fluid motion and thus decreases the velocity of the fluid. Figure 7 is plotted to show the trend of the porosity parameter (k_0) on the velocity profile. It is reported that the fluid velocity dwindles for the mounting estimation of (k_0). Physically, the motion of the fluid is hindered due to the presence of porous media, which is why a reduced velocity profile is witnessed. In Figure 8, a variation of heat absorption/generation coefficient (Q_0) on the temperature distribution is plotted. For rising estimates of Q_0, a higher temperature profile is observed. Figure 9 depicts the attributes of M_e on the temperature. It is examined that with an increase in values of M_e, the temperature profile reduces due to enhancement in thermal boundary layer thickness. Moreover, a sheet on normal temperature when dipped in the hot water. This causes the temperature to decrease while melting heat values may increase. The impact of Prandtl number (Pr) on the temperature profile is depicted in Figure 10. The increasing estimations of Pr results in a reduction of temperature field. Higher estimates of Prandtl number lower the thermal diffusivity, thus declining the temperature of the fluid. Figure 11 is illustrated to observe the behavior of non-linear chemical reaction (n) on the concentration profile. It is witnessed that the thickness of the species distribution increases as n increases. Figure 12 indicates the concentration profile for varying thermophoresis parameter (N_t). The temperature gradient is directly proportional to the larger values of N_t that, accordingly, upsurges the concentration profile and its related concentration boundary layer thickness. Figure 13 is designed to highlight the Schmidt number (S_c) behavior on the nanoparticle concentration $\phi(\eta)$. S_c is the ratio of momentum to the mass diffusion. For a growing estimation S_c, a reduction in the mass diffusion coefficient causes a thinner concentration boundary layer. The response of chemical reaction parameter (γ) on the concentration profile $\varphi(\eta)$ is observed in Figure 14. It is clearly examined that concentration $\varphi(\eta)$ is decreased via γ. In Figure 15, a retarding effect of λ against magnetic parameter M can be seen for skin friction. It is reported that the thinner boundary layer is accompanying larger values of λ, which results in a higher velocity gradient close to the wall. That is why drag force reduces against λ. An analysis of the impact λ and porosity parameter (k_0) on skin friction is detected in Figure 16. A dwindling effect of λ against k_0 can be noticed for skin friction.

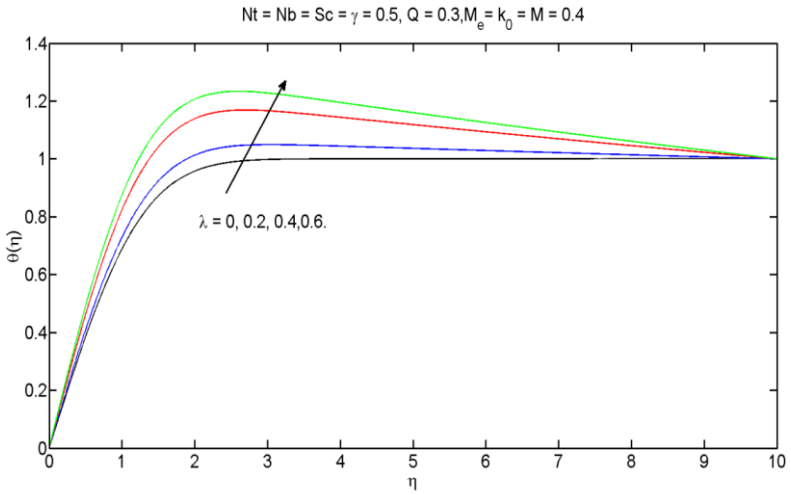

Figure 3. Illustration of $\theta(\eta)$ versus λ.

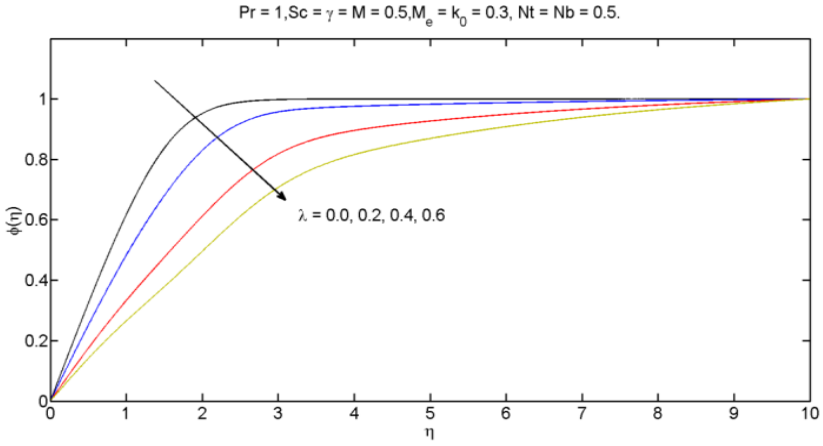

Figure 4. Illustration of $\varphi(\eta)$ versus λ.

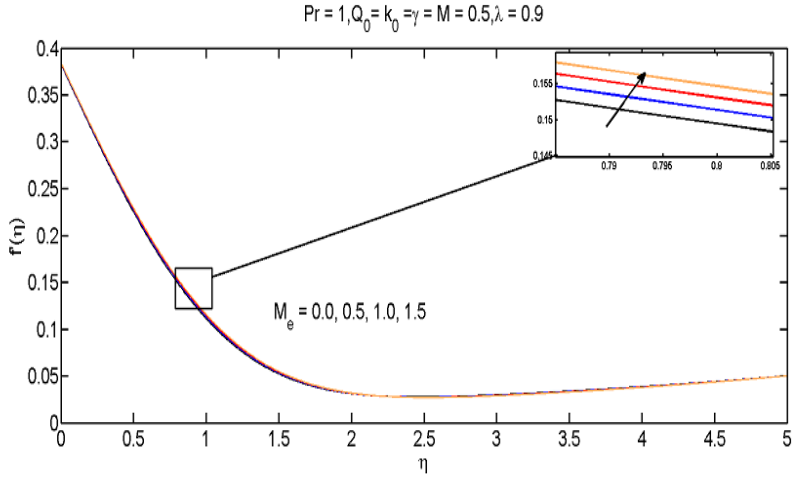

Figure 5. Illustration of $f'(\eta)$ versus M_e.

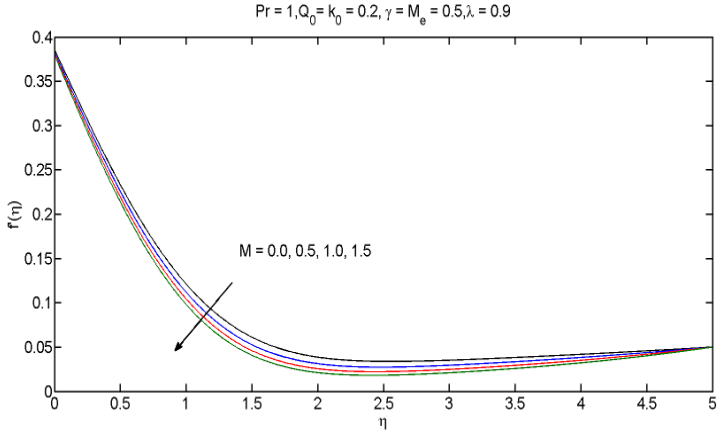

Figure 6. Illustration of $f'(\eta)$ versus M.

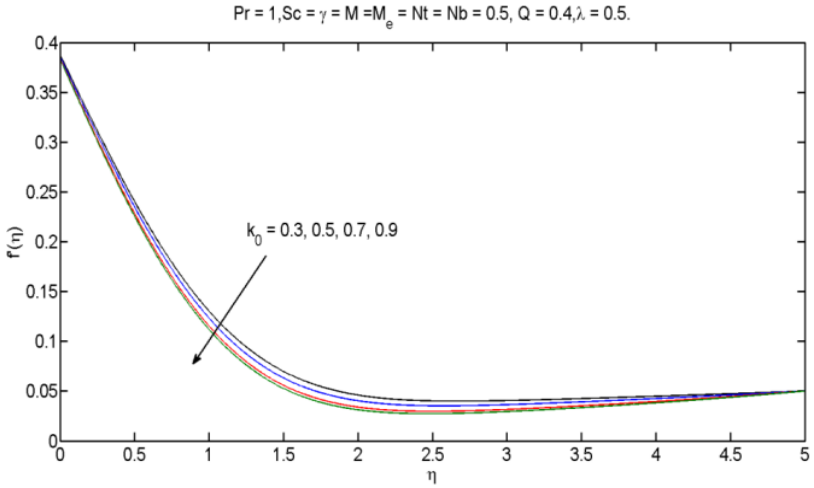

Figure 7. Illustration of $f'(\eta)$ versus k_0.

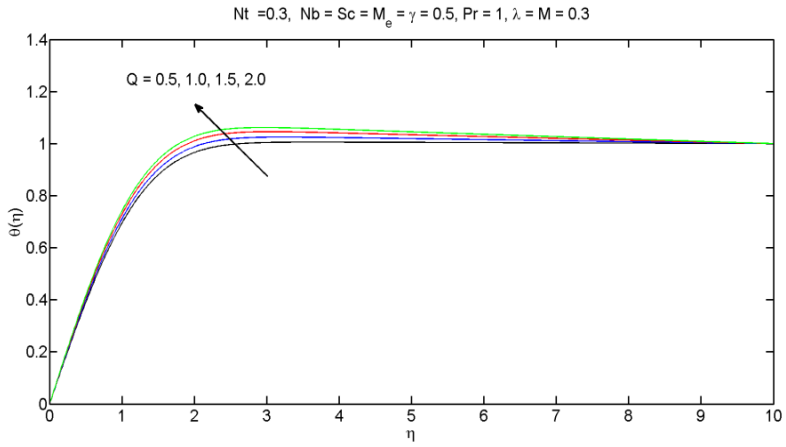

Figure 8. Illustration of $\theta(\eta)$ vs. Q.

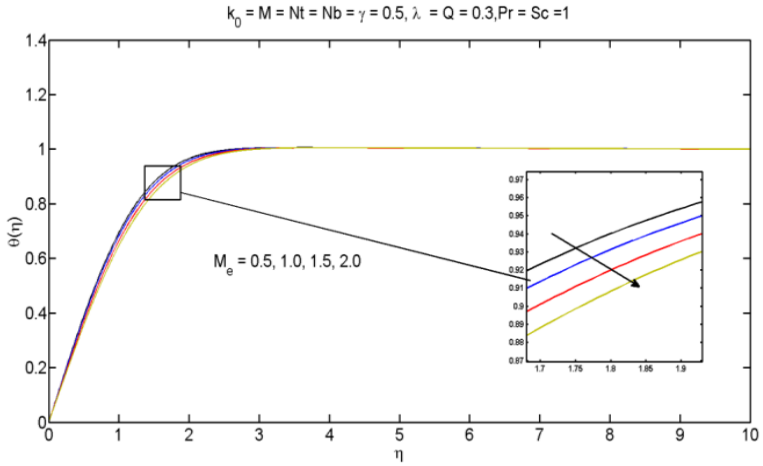

Figure 9. Illustration of $\theta(\eta)$ versus M_e.

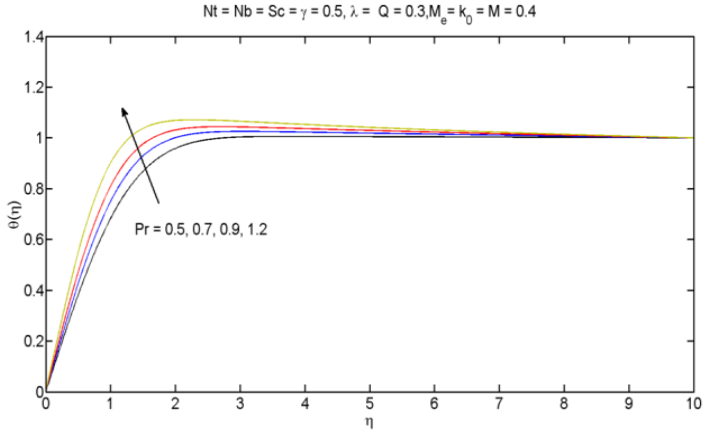

Figure 10. Illustration of $\theta(\eta)$ of vs. Pr.

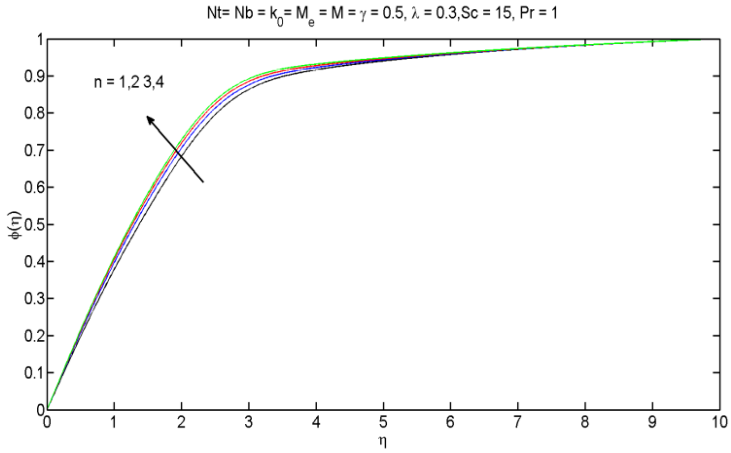

Figure 11. Illustration of $\varphi(\eta)$ versus n.

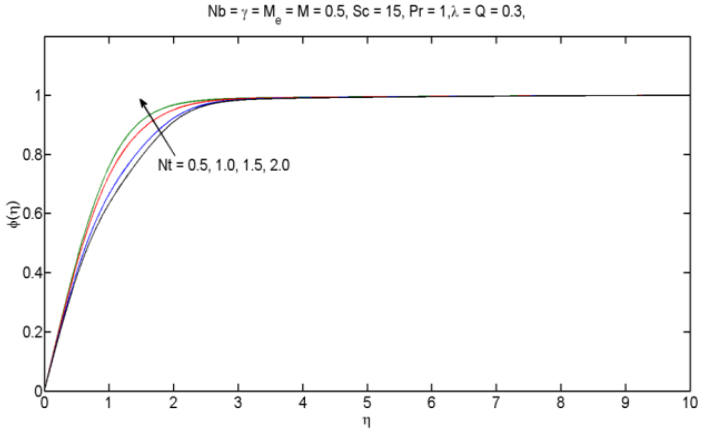

Figure 12. Illustration of $\varphi(\eta)$ versus N_t.

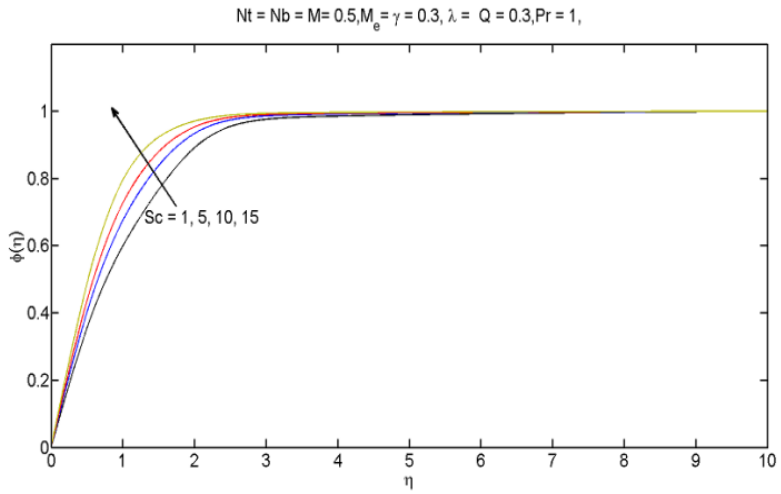

Figure 13. Illustration of $\varphi(\eta)$ versus Sc.

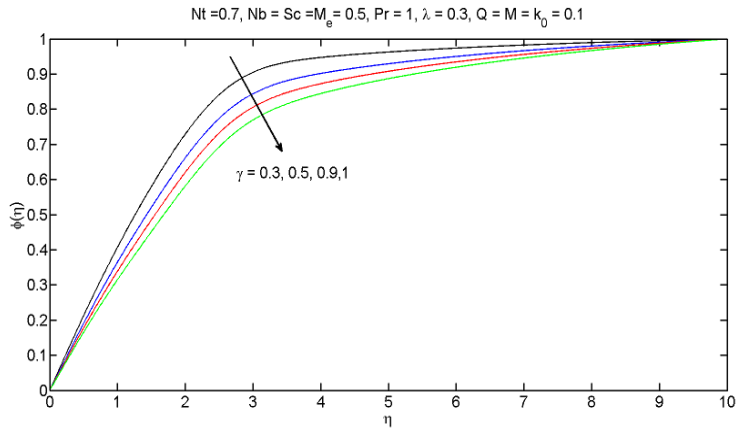

Figure 14. Illustration of $\varphi(\eta)$ versus γ.

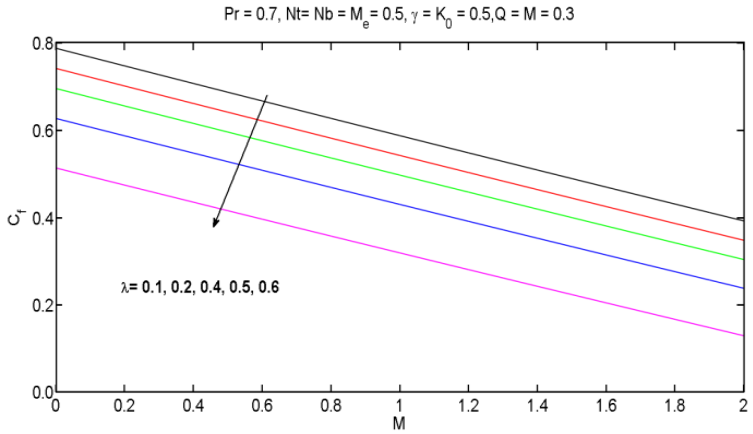

Figure 15. Illustration of skin friction coefficient versus λ and M.

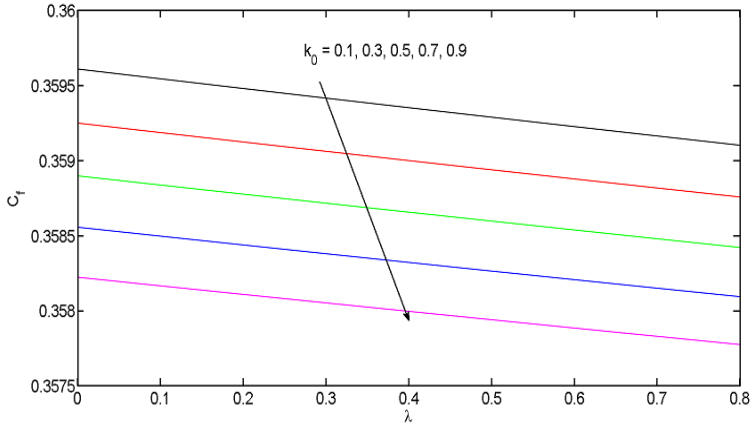

Figure 16. Illustration of skin friction coefficient versus k_0 and λ.

Table 1 portrays the values of $f''(m)$ with those of Ishak et al. [30] and Rida et al. [31] when $\lambda = 0$. An excellent consensus is achieved in this regard. Table 2 displays the behavior of different parameters such as M, λ, Q, Pr, m, N_t. on the local Nusselt number. It is witnessed that the rate of heat transfer enhances for a larger estimation of λ. The increasing values of λ show that the rate of cooling of the needle can be improved by reducing the external flow velocity or by enhancing the needle velocity. It is analyzed that the heat transfer rate is proportional to the values of Prandtl (Pr). It enhances for the growing values of Prandtl number. It is further reported that viscosity of the fluid is escalated as Pr increases. It is depicted that the heat transfer rate declines for peak estimation of thermophoresis parameter (N_t). Pr is a ratio of the momentum to thermal diffusivity. For increasing values of N_t, a heated needle with an opposite trend for negative values of N_t is observed. The next four entries show that the Nusselt number is enhanced when the needle size (m) is reduced from 0.1 to 0.001. For increased values of heat absorption/generation coefficient (Q_0), the Nusselt number increases.

Table 1. Comparison of $f''(m)$ with those of Ishak et al. [30] and Rida et al. [31] when $\lambda = 1$.

m	[30]	[31]	Current
0.10	01.2888	01.2888171	01.2888195
0.010	08.4924	08.4924360	08.4924451
0.0010	062.1637	062.163672	062.163674

Table 2. Values of the heat transfer rate for different parameters M, λ, Q, m, Pr, N_t.

λ	M	Pr	N_t	m	Q	
0						0.512632
0.1						0.517194
0.2						0.521715
0.3						0.526048
0.5						0.534528
0.5	0.5					0.513641
	1.0					0.503333
	1.5					0.499032
	2.0					0.464898
	2.5					0.489685
	0.5	0.1				0.526048
		0.2				0.55381
		0.3				0.580151
		0.4				0.606128

Table 2. *Cont.*

λ	M	Pr	N_t	m	Q	
		0.4	0.3			0.524781
			0.5			0.526048
			0.7			0.527304
			0.9			0.528548
			0.5	0.1		0.526048
				0.2		0.729278
				0.3		0.885838
				0.4		0.952821
				0.1	0.5	0.526048
					0.7	0.532366
					0.9	0.538761
					1.0	0.541987

5. Conclusions

We consider an incompressible steady MHD nanofluid flow over a thin needle immersed in permeable media and viscous dissipation in the existence temperature-dependent heat source/sink. The effects of melting heat transfer slip boundary condition and non-linear chemical reaction are also discussed. The conclusive remarks of the current study are presented as follows:

- Magnetic parameter (M) and porosity parameter (k_0) have a diminishing effect on radial velocity;
- Melting heat parameter (M_e) has a retarding effect on temperature profile while radial velocity enhances due to melting;
- Concentration profile increases for the mounting estimation of the Schmidt number;
- Concentration profile reduces for larger values of thermophoresis parameter (N_t) and chemical reaction parameter (γ),whereas it illustrates an opposite effect with upsurge values of a nonlinear chemical reaction (n);
- Drag force reduces for a large estimation of λ, magnetic parameter (M), and porosity parameter (k_0);
- Heat transfer rate depicts an escalating behavior for a higher value of λ, Q, Pr, m, N_t and opposite response for enlarge values of melting heat parameter (M_e).

Author Contributions: Conceptualization, M.R.; methodology, H.G.; software, S.K.; validation, S.K. and C.L.; formal analysis, H.G.; investigation, Y.N.; writing—original draft preparation, H.G.; writing—review and editing, F.H.; supervision, M.R.; project administration, M.R.; funding acquisition, Y.N.

Funding: This work was supported by the Soonchunhyang University Research Fund.

Acknowledgments: This research was supported by Basic Science Research Program through the National Research Foundation of Korea (NRF) funded by the Ministry of Education (NRF-2017R1D1A3B03028309) and also supported by the Soonchunhyang University Research Fund.

Conflicts of Interest: The authors declare no conflicts of interest regarding this publication.

Nomenclature

M	Magnetic parameter
C	Concentration of fluid
Q	Heat absorption coefficient
Pr	Prandtl number
D_B	Brownian diffusion coefficient
ρ	Density of liquid
u_w	Uniform velocity
M_e	Melting heat
T_m	Wall temperature
u_s	Stretching velocity

ν	Kinematic viscosity
C	Nanoparticle concentration
D_T	Thermophoretic diffusion
U	Composite velocity
k_n	Coefficient of chemical reaction
$\boldsymbol{T_0}$	Reference temperature
L	Velocity slip factor
S_1	Constant
λ	Velocity ratio parameter
m	Needle size parameter
N_t	Thermophoresis parameter
N_b	Parameter of Brownian motion
γ	Chemical reaction parameter
Sc	Schmidt number
$\boldsymbol{Re_x}$	Reynolds number
T_∞	Ambient temperature
T	Nanofluid temperature
u_∞	Stream velocity
C_m	Wall concentration
C_∞	Ambient concentration
u, v	Components of Velocities
σ	Stefan–Boltzmann
α	Thermal diffusivity
$\boldsymbol{c_p}$	Capacity of Specific heat
$\boldsymbol{B_0}$	Strength of Magnetic field
λ_1	Latent heat of fluid
k^*	Permeability of spongy medium

References

1. Hayat, T.; Imtiaz, M.; Alsaedi, A. Unsteady flow of nanofluid with double stratification and magnetohydrodynamics. *Int. J. Heat Mass Transf.* **2016**, *92*, 100–109. [CrossRef]
2. Ramzan, M.; Gul, H.; Chung, J.D. Double stratified radiative Jeffery magneto nanofluid flow along an inclined stretched cylinder with chemical reaction and slip condition. *Eur. Phys. J. Plus* **2017**, *132*, 456. [CrossRef]
3. Ellahi, R. The effects of MHD and temperature dependent viscosity on the flow of non-Newtonian nanofluid in a pipe: Analytical solutions. *Appl. Math. Model.* **2013**, *37*, 1451–1467. [CrossRef]
4. Ramzan, M. Influence of Newtonian heating on three dimensional MHD flow of couple stress nanofluid with viscous dissipation and joule heating. *PLoS ONE* **2015**, *10*, e0124699. [CrossRef] [PubMed]
5. Ramzan, M.; Farooq, M.; Hayat, T.; Chung, J.D. Radiative and Joule heating effects in the MHD flow of a micropolar fluid with partial slip and convective boundary condition. *J. Mol. Liq.* **2016**, *221*, 394–400. [CrossRef]
6. Bin-Mohsin, B. Buoyancy Effects on MHD Transport of Nanofluid over a Stretching Surface with Variable Viscosity. *IEEE Access* **2019**, *7*, 75398–75406. [CrossRef]
7. Sheikholeslami, M.; Shah, Z.; Tassaddiq, A.; Shafee, A.; Khan, I. Application of Electric Field for Augmentation of Ferrofluid Heat Transfer in an Enclosure Including Double Moving Walls. *IEEE Access* **2019**, *7*, 21048–21056. [CrossRef]
8. Choi, S.U.S.; Eastman, J.A. Enhancing thermal conductivity of fluids with nanoparticles. *ASME Publ. Fed* **1995**, *231*, 99–106.
9. Kang, H.U.; Kim, S.H.; Oh, J.M. Estimation of thermal conductivity of nanofluid using experimental effective particle volume. *Exp. Heat Transf.* **2006**, *19*, 181–191. [CrossRef]
10. Jafaryar, M.; Sheikholeslami, M.; Li, Z.; Moradi, R. Nanofluid turbulent flow in a pipe under the effect of twisted tape with alternate axis. *J. Therm. Anal. Calorim.* **2019**, *135*, 305–323. [CrossRef]
11. Hayat, T.; Khan, M.I.; Farooq, M.; Yasmeen, T.; Alsaedi, A. Water-carbon nanofluid flow with variable heat flux by a thin needle. *J. Mol. Liq.* **2016**, *224*, 786–791. [CrossRef]

12. Khan, M.W.A.; Khan, M.I.; Hayat, T.; Alsaedi, A. Entropy generation minimization (EGM) of nanofluid flow by a thin moving needle with nonlinear thermal radiation. *Phys. B Condens. Matter* **2018**, *534*, 113–119. [CrossRef]
13. Sulochana, C.; Ashwinkumar, G.P.; Sandeep, N. Joule heating effect on a continuously moving thin needle in MHD Sakiadis flow with thermophoresis and Brownian moment. *Eur. Phys. J. Plus* **2017**, *132*, 387. [CrossRef]
14. Trimbitas, R.; Grosan, T.; Pop, I. Mixed convection boundary layer flow along vertical thin needles in nanofluids. *Int. J. Numer. Methods Heat Fluid Flow* **2014**, *24*, 579–594. [CrossRef]
15. Sulochana, C.; Samrat, S.P.; Sandeep, N. Boundary layer analysis of an incessant moving needle in MHD radiative nanofluid with joule heating. *Int. J. Mech. Sci.* **2017**, *128*, 326–331. [CrossRef]
16. Salleh, S.; Bachok, N.; Arifin, N.; Ali, F.; Pop, I. Stability analysis of mixed convection flow towards a moving thin needle in nanofluid. *Appl. Sci.* **2018**, *8*, 842. [CrossRef]
17. Khaled, A.R.; Vafai, K. The effect of the slip condition on Stokes and Couette flows due to an oscillating wall: Exact solutions. *Int. J. Non Linear Mech.* **2004**, *39*, 795–809. [CrossRef]
18. Wang, C.Y.; Ng, C.O. Slip flow due to a stretching cylinder. *Int. J. Non Linear Mech.* **2011**, *46*, 1191–1194. [CrossRef]
19. Khader, M.M.; Megahed, A.M. Numerical solution for boundary layer flow due to a nonlinearly stretching sheet with variable thickness and slip velocity. *Eur. Phys. J. Plus* **2013**, *128*, 100. [CrossRef]
20. Bhattacharyya, K.; Mukhopadhyay, S.; Layek, G.C. Similarity solution of mixed convective boundary layer slip flow over a vertical plate. *Ain Shams Eng. J.* **2013**, *4*, 299–305. [CrossRef]
21. Sheikholeslami, M. CuO-water nanofluid flow due to magnetic field inside a porous media considering Brownian motion. *J. Mol. Liq.* **2018**, *249*, 921–929. [CrossRef]
22. Sheikholeslami, M. New computational approach for exergy and entropy analysis of nanofluid under the impact of Lorentz force through a porous media. *Comput. Methods Appl. Mech. Eng.* **2019**, *344*, 319–333. [CrossRef]
23. Li, Z.; Ramzan, M.; Shafee, A.; Saleem, S.; Al-Mdallal, Q.M.; Chamkha, A.J. Numerical approach for nanofluid transportation due to electric force in a porous enclosure. *Microsyst. Technol.* **2019**, *25*, 2501–2514. [CrossRef]
24. Sheikholeslami, M.; Shafee, A.; Ramzan, M.; Li, Z. Investigation of Lorentz forces and radiation impacts on nanofluid treatment in a porous semi annulus via Darcy law. *J. Mol. Liq.* **2018**, *272*, 8–14. [CrossRef]
25. Bilal, M.; Ramzan, M. Hall current effect on unsteady rotational flow of carbon nanotubes with dust particles and nonlinear thermal radiation in Darcy–Forchheimer porous media. *J. Therm. Anal. Calorim.* **2019**, *138*, 3127–3137. [CrossRef]
26. Roberts, L. On the melting of a semi-infinite body of ice placed in a hot stream of air. *J. Fluid Mech.* **1958**, *4*, 505–528. [CrossRef]
27. Hayat, T.; Farooq, M.; Alsaedi, A. Melting heat transfer in the stagnation-point flow of Maxwell fluid with double-diffusive convection. *Int. J. Numer. Methods Heat Fluid Flow* **2014**, *24*, 760–774. [CrossRef]
28. Das, K. Radiation and melting effects on MHD boundary layer flow over a moving surface. *Ain Shams Eng. J.* **2014**, *5*, 1207–1214. [CrossRef]
29. Mabood, F.; Mastroberardino, A. Melting heat transfer on MHD convective flow of a nanofluid over a stretching sheet with viscous dissipation and second order slip. *J. Taiwan Inst. Chem. Eng.* **2015**, *57*, 62–68. [CrossRef]
30. Ishak, A.; Nazar, R.; Pop, I. Boundary layer flow over a continuously moving thin needle in a parallel free stream. *Chin. Phys. Lett.* **2007**, *24*, 2895. [CrossRef]
31. Ahmad, R.; Mustafa, M.; Hina, S. Buongiorno's model for fluid flow around a moving thin needle in a flowing nanofluid: A numerical study. *Chin. J. Phys.* **2017**, *55*, 1264–1274. [CrossRef]